AD-A056 662 NORTHWESTERN UNIV EVANSTON IL DEPT OF MATERIALS SCIENCE F/G 14/2
GEOMETRICAL PROBLEMS WITH A POSITION SENSITIVE DETECTOR EMPLOYE--ETC(U)
JUN 78 M R JAMES, J B COHEN N00014-75-C-0580
UNCLASSIFIED TR-20 NL

1 OF 1
AD A056662

END
DATE FILMED
9-78
DDC

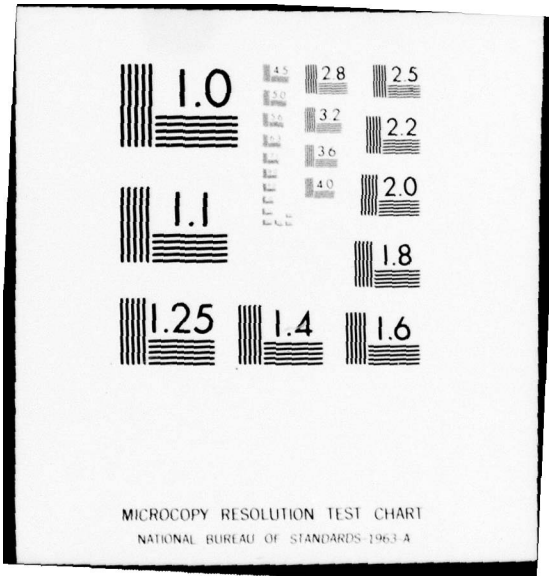
1.0
1.1
1.25
1.4
1.6
2.0
2.2
2.5
2.8
3.2
3.6
4.0
4.5
5.0
MICROCOPY RESOLUTION TEST CHART
NATIONAL BUREAU OF STANDARDS-1963-A

LEVEL II

(12)

NORTHWESTERN UNIVERSITY

DEPARTMENT OF MATERIALS SCIENCE

(9) Technical Report No. 20
June 16, 1978

(14) TR-20

(15) Office of Naval Research
Contract N00014-75-C-0580
NR 031-733

(6) GEOMETRICAL PROBLEMS WITH A POSITION SENSITIVE DETECTOR EMPLOYED ON A DIFFRACTOMETER, INCLUDING ITS USE IN THE MEASUREMENT OF STRESS.

by

(14) M. R. James and J. B. Cohen
Michael
Jerome

(11) 16 Jun 78

(12) 29 p.

NORTHWESTERN UNIVERSITY QUAECUMQUE SUNT VERA 1851 ὁ λόγος καὶ ἡ ἀλήθεια θείας

EVANSTON, ILLINOIS

260 814

ACH

GEOMETRICAL PROBLEMS WITH A POSITION SENSITIVE DETECTOR EMPLOYED ON A DIFFRACTOMETER, INCLUDING ITS USE IN THE MEASUREMENT OF STRESS

M. R. James[o] and J. B. Cohen
Dept. of Materials Science and Engineering
The Technological Institute
Northwestern University
Evanston, Illinois 60201

ABSTRACT

Defocusing errors associated with the use of a straight one dimensional position sensitive detector on a powder diffractometer are examined. At high angles, the error is less than the resolution of currently available detectors for x-rays.

1. INTRODUCTION

Commercial position sensitive detectors (PSD) for x-rays (Borkowski and Kopp, 1968) are effectively long, straight wires. The delay time of the signal to both ends of the wire from one position is converted to voltage which allows simultaneous storage of a wide angular range in a multi-channel analyzer (typically $\approx 20 - 30^{o}$ 2θ) with a position resolution of $\approx 60\ \mu - 180\ \mu$. With parafocusing geometry the entire detector length cannot be located on the focusing circle. Only that portion of the detector tangent to the circle will be at the true focusing position. (Also, the dimensions of most present commercial PSD's prohibit their location on the focusing circle at high angles, greater than $140^{o}2\theta$, because the PSD is

[o] Currently at Rockwell International Science Center, 1049 Camino Dos Rios, Thousand Oaks, California 91360, U.S.A.

obstructed by the x-ray source on most diffractometers.)

It is the purpose of this paper to explore the errors associated with this problem which are relevant to their general use on a diffractometer as well as in x-ray measurements of residual stress.

The measurement of residual stress in the surface of materials is generally carried out by tilting a specimen to an incident x-ray beam one or more ψ values (about an axis normal to the diffracting plane) on some form of a diffractometer and measuring the peak shift; see for example Cullity (1978) for a review of the method. Recently, it has been shown that the time for these measurements can be greatly decreased by using a linear position sensitive detector (James and Cohen, 1976, 1977, 1978).

In general a modified form of Seeman-Bohlin geometrical conditions for focusing is employed. This permits a divergent primary beam and hence illumination of a considerable area of the specimen, yet results in a sharp diffracted beam at the focal point. The focusing circle defined by the target, specimen and receiving slit, as shown in Fig. 1, is related to the radius of the diffractometer circle, R_{GC}, as follows (SAE, 1971).

$$R_{FC} = R_{GC}/2\sin(\theta + \psi) \qquad (1a)$$

Where ψ is defined in Fig. 1.b. Fig. 1 illustrates two possible conditions. For $\psi = 0$, the focal point lies on the goniometer circle at all 2θ angles. This is the usual Bragg-Brentano focusing. A receiving slit placed on the 2θ arm at the position of the goniometer circle is always at the point of focus. For ψ not equal to zero, the

point of focus changes to point B in Fig. 1.b. The distance from the sample to B is given by Cullity (1978):

$$R_P = (R_{GC}) \frac{\cos(\psi+(90-\theta))}{\cos(\psi-(90-\theta))} . \qquad (1b)$$

Equation (1b) is valid for either a positive or negative ψ tilt. The counter and/or receiving slit may be moved to this position in the x-ray measurement of residual stress.

2. GEOMETRIC ERROR

Referring to Fig. 2, the angle 2φ is given by:

$$2\varphi = \tan^{-1}(\frac{nz}{R}), \qquad (2a)$$

where nz is the length along the PSD from a reference position, q (which is the point of tangency of the detector to the focusing circle). Define a calibration k:

$$k = \frac{\alpha}{z} \qquad (2b)$$

where α is the angle determining the distance z, which can be made equal to one channel. (Hence the units of k are $^{\circ}2\theta$/channel.) Thus:

$$2\varphi = \tan^{-1}(n \tan kz). \qquad (2c)$$

Calibration is achieved by examining any two peaks (such as a doublet), within the range of the PSD with fixed settings of the PSD electronics, and with a normal diffractometer. (In our laboratory, with 1024 channels, a typical value of k is $0.0202^{\circ}2\theta$ per channel.)

The true 2θ is then:

$$2\theta_o + 2\varphi \qquad (2d)$$

where $2\theta_o$ is the value at q. A comparison was made between this equation and:

$$2\theta = 2\theta_o + k(nz) \qquad (2e)$$

The difference was less than $0.01^\circ 2\theta$ over $4.5^\circ 2\theta$ on either side of q, and $\approx 0.001^\circ 2\theta$ over $2.25^\circ 2\theta$.

3. DEFOCUSING ERROR

3.1 Treatment of Aberrations in the Diffraction Profile

Although a crystal will reflect over a small range of 2θ depending on the spectral dispersion of the primary beam, the crystallite size, microstrain, faults, etc., it will be assumed here that there is only one wavelength and that Bragg's law applies exactly; for any $(hk\ell)$ plane the diffraction angle is fixed.

A method developed by A. J. C. Wilson (1963) to study aberrations arising from the practical impossibility of achieving the ideal arrangement in powder diffractometry will be followed. Wilson's purpose for treating these aberrations was to determine what could be done to eliminate, as far as practicable, the effect of the aberrations on the observed positions, breadths and profiles of diffraction maxima. In this paper, it is desired solely to determine if aberrations due to defocusing cause errors in the measurement of peak position using a position sensitive detector.

Wilson's treatment involves aberrations such as horizontal divergence, specimen shape, specimen transparency to the x-ray beam, receiving slit position, etc. on the measured Bragg angle. In this paper, we only need to be concerned with the effect of the receiving position on the measured Bragg angle.

Fig. 3. illustrates the geometry of the approach. A ray diverging from point C, a distance $\bar{X}_f$ from A, the centroid of the source, is diffracted at point P in the specimen a distance $\bar{X}_s$ from 0 (the ideal position of the specimen) and passes through the receiving slit at D, at distance $\bar{X}_r$ from B, the point at which rays would be focused under ideal conditions. The main concern with a PSD is with errors associated with the vector $\bar{X}_r$. The other errors are included because of possible cross terms involving $\bar{X}_f$ and $\bar{X}_s$.

Following Wilson's coordinate system, unit vectors may be chosen with $\tilde{I}$ and $\tilde{J}$ in the diffracting plane, $\tilde{i}$ radially outward from the focusing circle, $\tilde{j}$ tangential to the focusing circle, and $\tilde{k}$ axial. The $\tilde{X}$ direction is thus normal to the circle and $\tilde{Y}$ and $\tilde{Z}$ are tangential to it. Orthogonal components for the vectors $\bar{X}_f$, $\bar{X}_s$. $\bar{X}_r$ may be chosen so that:

i) x_s, y_s, z_s are parallel to $\tilde{I}$, $\tilde{J}$, $\tilde{K}$,

ii) x_f, and y_f are equatorial and respectively parallel and perpendicular to the incident beam in Fig. 3 and z_f is parallel to $\tilde{k}$,

iii) x_r, and y_r are equatorial and respectively parallel and perpendicular to $\bar{R}$, and z_r is parallel to $\tilde{k}$.

Let 2ε represent the error in the value, 2θ, due to the aberrations. Then:

$$2\theta = 2\varphi + 2\varepsilon \tag{3}$$

where the angular reading on the diffractometer is actually 2φ. To calculate 2ε:

$$\cos 2\varphi - \cos 2\theta = \cos 2\varphi - \cos(2\varphi + 2\varepsilon)$$

$$\cong 2\varepsilon \sin 2\varphi \tag{4a}$$

or:

$$2\varepsilon = [\cos 2\varphi - \cos 2\theta]/\sin 2\varphi \tag{4b}$$

where 2ε is in radians. Letting $\cos 2\varphi - \cos 2\theta = \delta$ this term can be separated into its components:

$$\delta = \delta_f + \delta_r + \delta_s + \delta_{fr} + \delta_{fs} + \delta_{rs}, \tag{5}$$

where δ_f, δ_r, δ_s represent the scalar components involving only the focal spot, receiving slit, and specimen respectively. δ_{fr}, δ_{fs}, and δ_{rs} are cross terms involving the designated constituents. These cross terms represent the correlations of one aberration with another. For instance, if the focal spot and effective diffracting position were perfectly positioned with the angular divergence of the beam being extremely small, there would be no receiving slit missetting because the diffracted beam would be a straight line. The correlation of errors associated with the finite sizes and locations of the focal spot and receiving slit, and volume and receiving slit must be taken into account. As the present concern

is only with terms involving the receiving slit:

$$\delta = \delta_r + \delta_{fr} + \delta_{rs}. \tag{6}$$

The scalar terms as derived by Wilson are:

$$\delta_r = R^{-2}\sin 2\varphi\left[Ry_r - x_r y_r + \tfrac{1}{2}(y_r^2 + z_r^2)\cot 2\varphi + \ldots\right], \tag{7a}$$

$$\delta_{fr} = (RS)^{-1}(y_f y_r \cos 2\varphi + z_f z_r), \tag{7b}$$

$$\delta_{rs} = R^{-2}\left[-x_r x_s \cos(2\varphi-\psi)\sin 2\varphi - y_r y_s \cos(2\varphi-\psi)\sin 2\varphi\right. \tag{7c}$$

$$\left. -x_r y_s \sin(2\varphi-\psi)\sin 2\varphi - z_r z_s(\cos 2\varphi + \frac{R}{S}) + -y_r x_s(\cos\psi + \frac{R}{S}\cos\psi\cos 2\varphi)\right].$$

We neglect the axial divergence terms because the PSD slit height is 3mm (equal to 1.2° for a diffractometer of radius 14.55 cm), small compared to a normal receiving slit and we are interested in errors different than the usual slit arrangement. The displacement is found by averaging $2\epsilon_r$ over the focal spot, specimen, and receiving slit. Neither x_r and x_s, nor x_r and y_s, nor y_f and y_r, are correlated; thus:

$$2\epsilon_r = R^{-2}\left[R\langle y_r\rangle - \langle x_r\rangle\langle y_r\rangle + \frac{\langle y_r^2\rangle}{2}\cot 2\varphi - \langle x_r\rangle\langle x_s\rangle\cos(2\varphi-\psi)\right.$$

$$- \langle y_r\rangle\langle y_s\rangle\cos(2\varphi-\psi) - \langle x_r\rangle\langle y_s\rangle\sin(2\varphi-\psi) - \frac{\langle y_r\rangle\langle x_s\rangle}{\sin 2\varphi}(\cos\psi + \frac{R}{S}\cos\psi\cos 2\varphi)$$

$$\left. + \frac{R}{S}\langle y_r\rangle\langle y_f\rangle\cot 2\varphi)\right] \tag{8}$$

where $\langle x_r y_r\rangle = \langle x_r\rangle\langle y_r\rangle$ is assumed. The term $\langle x_s\rangle$ will be taken as the displacement of the effective center of the diffracting volume of a flat specimen from the diffractometer's center point. If the center of gravity of the illuminated area lies on the axis of rotation of the specimen, $\langle y_s\rangle = 0$. This is never possible because of the

variation in intensity across the beam, but the average is generally still small. Both x_r and y_r will be functions of 2φ and the position of the PSD.

3.2 Derivation of $\langle x_r \rangle$ and $\langle y_r \rangle$

In the coordinate system for $\bar{X}_r$, x_r is the distance between the ideal focal point given by Eq. (1b) and the detector in the direction parallel to R. In addition, y_r is defined as being perpendicular to R and dependent on the divergence of the primary beam. It arises because even if the focal spot were a point, as shown in Fig. 1b, the rays diverge again before being detected. The centroid of this distribution will not be in the center of the divergent beam creating an aberration in the measured distribution. An estimate of both these quantities can be made following a method presented by H. Zantopulos and C. F. Jatczak (1970). Equations are derived in this reference for the path of the incident and diffracted beams. Defining the position of the PSD by an equation in the same coordinate system, the intersection of the diffracted beam and the PSD can be specified. The distance from the focus, point B in Fig. 1b, to the intersection of the diffracted ray and the PSD can then be determined, and x_r and y_r found.

The origin, 0, in Fig. 4, is the axis of rotation of the specimen and the Cartesian coordinates i, j define the equatorial plane. Assuming a flat sample, a primary beam divergence of 2α, and 2φ as the observed Bragg angle, these equations will be derived below.

3.2A Equation for the Incident Beam

In Fig. 4, the slope of the central incident beam is given by $-\cot\beta$, where $\beta = 90-\varphi$. Using the law of sines in the triangle AOB to find the j axis intercept, the equations for the right and left incident beam are, respectively:

$$j = -\cot(\beta-\alpha)i + R\sin\alpha/\sin(\beta-\alpha), \tag{9a}$$

$$j = -\cot(\beta+\alpha)i - R\sin\alpha/\sin(\beta+\alpha).$$

To generalize, let:

$\ell = 1$ for the right beam,

$\ell = 0$ for the central beam,

$\ell = -1$ for the left beam.

Then the equation for the incident beam becomes:

$$j = -\cot(\beta-\ell\alpha)i + \ell R\sin\alpha/\sin(\beta-\ell\alpha). \tag{9b}$$

Note that α is half the divergence angle.

3.2B. Intersection of Incident Beam and Specimen Surface

The specimen surface can be defined by:

$$j = i\tan\psi, \tag{10}$$

where ψ is defined in Fig. 1. Equating Eqs. 9b and 10, the coordinates of the intersections are:

$$i_s = \frac{\ell R\sin\alpha/\sin(\beta-\ell\alpha)}{[\cot(\beta-\ell\alpha)+\tan\psi]}, \tag{11a}$$

$$j_s = i_s\tan\psi. \tag{11b}$$

The subscript s in Eqs. 11 refers to the intersection of the incident beam and specimen.

3.2C Equations for the Diffracted Beam

The slope of the diffracted beam is given by $\cot(\beta+l\alpha)$. Fig. 4 defines the j axis intercept for the left and right beam. For the diffracted beam:

$$j = \cot(\beta+l\alpha)i - i_s\tan(\beta+l\alpha) \tag{12}$$

3.2D Intersection of the Diffracted Beam and the PSD

It is convenient to describe the position of the PSD by the point at which it is tangent to the focusing circle, D_2 in Fig. 5. The angle between the line connecting D_2 and the origin and the j axis can be described by β'. The equation of the line passing through D_2 and the origin is:

$$j = (\cot\beta')i \tag{13}$$

The PSD is perpendicular to the $0\text{-}D_2$ and, therefore, the line representing the PSD has a slope of $-\tan\beta'$. The intercept of the line on which the PSD lies and the j axis is $-R/\cos\beta'$ as seen in Fig. 5. The equation for the line on which the PSD lies is then given by:

$$j = -i\tan\beta' - R/\cos\beta'. \tag{14}$$

The simultaneous solution of Eq. 12 and Eq. 14 yields the coordinates of D1 (the intersection of any diffracted beam and the PSD):

$$i_D = (i_s\tan(\beta+l\alpha)-R/\cos\beta')(1/(\cot(\beta+l\alpha)+\tan\beta')), \tag{15a}$$

$$j_D = -i_D\tan\beta' - R/\cos\beta'. \tag{15b}$$

The distance from the sample to the detector is given by:

$$R_{PSD} + (i_D^2 + j_D^2)^{\frac{1}{2}}. \tag{16}$$

Fig. 6 illustrates the error in x_r which has been defined as being parallel to R. The magnitude of x_r for the left, central, and right beams are almost identical as the divergence angle is small. The distance from the focal point B, given by Eq. (1b) and the intersection of the beam on the PSD is given by:

$$x_r \simeq R_{PSD} - R_P = (i_D^2 + j_D^2)^{\frac{1}{2}} - R\frac{\cos(\psi+\beta)}{\cos(\psi-\beta)}, \tag{17}$$

where i_D and j_D are calculated for the central beam.

Defining β_L as the angle between the origin and a line connecting the origin with the intersection of the left beam and the PSD and β_R similarly corresponding to the right beam, then from Fig. 7:

$$2\varphi_L = 180-\beta_L-\beta_c, \tag{18a}$$

$$2\varphi_R = 180-\beta_R-\beta_c, \tag{18b}$$

where $\beta_i = \tan^{-1}(i_D/j_D)$ using the appropriate values of i and j from Eq. 15 and Eq. 16. The average error is given by the difference between the angle of the central beam, $2\varphi_c$, and the midpoint of the two extreme rays:

$$\Delta 2\varphi = 2\varphi_c - (2\varphi_L + 2\varphi_R)/2. \tag{19}$$

An average value of y_r is given by:

$$\langle y_r \rangle = R_p \tan\Delta 2\varphi. \tag{20}$$

Zantopulos and Jactzak (1970) have shown that the proper value is closer to 1/3 of this average, because the beam decreases in intensity rapidly on its edges. Eq. 20 is a liberal estimate.

4. EXAMPLES OF RESULTANT ERRORS

The defocusing error is given by Eq. 8. The terms x_r and y_r pertaining to the distance of the PSD from the focusing circle are given by Eq. 17 and 20 respectively. The remaining terms $\langle x_s \rangle$, $\langle y_f \rangle$ and $\langle y_s \rangle$ account for the interaction between the defocusing and sample position and a reasonable estimate of each must be used to determine the defocusing error. An estimate of $\langle y_s \rangle$ is difficult as it depends on the alignment; however, Wilson (1963) suggests a value of .25mm as the upper boundary. The term $\langle x_s \rangle$ represents the point of diffraction in the specimen, including both beam penetration and sample missetting; .05 mm representing an upper limit for most x-radiations. The term $\langle y_f \rangle$ is the missetting of the centroid of the primary illumination of the target from its true point on the focusing circle and is judged to be less than .05 mm.

The defocusing error was first calculated assuming the center of the PSD is tangent to the $\psi = 0^\circ$ focusing circle (goniometer radius = 14.55 cm) at $156^\circ 2\theta$, a typical value for stress measurement with steels. Table 1 tabulates the error assuming $\langle x_s \rangle$, $\langle y_s \rangle$ and $\langle y_f \rangle$ are zero. The true diffraction angle 2θ, as given by Eq. 3, is recorded for three values of α where the observed angle 2ϕ is 150°, 156° and $160^\circ 2\theta$. The error at the observed angle of $156^\circ 2\theta$, i.e. the tangency point of the detector and the focusing circle arises from the flat sample geometry and would be evident even with the usual receiving slit geometry. This error is comparable with those calculated by Zantopulos and Jatczak for stationary slit geometry.

The error due to the PSD only may be found by comparing the error at the point of tangency to that at 150° or $160^{\circ}2\theta$; this difference is very small. In terms of a stress measurement, for a peak shift, from $154^{\circ}2\theta$ at $\psi = 0^{\circ}$ to $156^{\circ}2\theta$ at $\psi = 45^{\circ}$, representing a stress of approximately -1200 MPa (-170,000 psi), the error due to defocussing is only +3 MPa (+430 psi) for a beam divergence (2α) of 2°:

Table 2 tabulates the error for $\langle x_s \rangle = \langle y_f \rangle = .05$ mm and $\langle y_s \rangle = .05$ mm. In this case, the defocusing errors are larger, especially at $\psi = 60^{\circ}$ because of the correlation between the specimen and beam missettings with the receiving slit missetting. Assuming the same 2° peak shift as before, the error in the peak shift between $\psi = 0^{\circ}$ and $\psi = 45^{\circ}$ is - 7.1 MPa (-1032 psi) still a small error considering the large peak shift.

From Eq. 8 it can be seen that $\langle x_s \rangle$ is most important at $\psi = 0$ where the cosine term is large. The effect is small though; for $\langle x_s \rangle = .05$ ($\langle y_f \rangle = \langle y_s \rangle = 0$), $2\varphi = 150$, $\alpha = .5^{\circ}$ and the detector tangent at $156^{\circ}2\theta$, the true diffraction angles are $149.998^{\circ}2\theta$ and $150.002^{\circ}2\theta$ at $\psi = 0$ and $\psi = 45^{\circ}$, respectively. The effect of $\langle y_f \rangle$ is similar in magnitude. However, the term $\langle y_s \rangle$ is more important. Because the quantity x_r is largest at $\psi \neq 0$, as is the sine term, $\langle y_s \rangle$ is most important at $\psi = \psi^{\circ}$. For $\langle y_s \rangle = .25$ mm ($\langle y_f \rangle = \langle x_s \rangle = 0$) and the above settings, the true diffraction angles are $149.998^{\circ}2\theta$ at $\psi = 0$ and 149.975 at $\psi = 45^{\circ}$. Most of the error recorded in Table 2 at $\psi \neq 0$ is, therefore, due to $\langle y_s \rangle$.

Table 3 tabulates the angles for $\langle x_s \rangle = \langle y_f \rangle = .05$ mm and $\langle y_s \rangle = .25$ mm, for the PSD being tangent to the $\psi = 0^\circ$ focusing circle at $139^\circ 2\theta$ (a typical diffraction angle for the CrK_α 311 diffraction plane in Al in stress measurements). The error is small for $\psi = 0$ but is quite large at $\psi = 45^\circ$ and $\psi = 60^\circ$. This is because the sine term is large at this angle, $2\varphi - \psi$, and involves $\langle y_s \rangle$. Assuming a peak shift from $139^\circ 2\theta$ to $141^\circ 2\theta$ using ψ tilts of 0° and 60° respectively, the error due to defocusing for Al, having a stress constant of 255 MPa/$^\circ 2\theta$ (3700 psi/$^\circ 2\theta$) is -8.67 MPa (-1240 psi) at a beam divergence of 2°. For $\langle y_s \rangle = 0$ the defocusing error is less than $.006^\circ 2\theta$ at $\psi = 45^\circ$. This effect is expected because at smaller 2θ the effective sample positioning and beam alignment are more critical.

Data is tabulated in Table 4 for 2φ angles less than 90°. Alignment errors become critical at these angles so values are reported for $\langle x_s \rangle = \langle y_s \rangle = \langle y_f \rangle = 0$, and beam divergences of 1° and 2°. It is readily seen that for the detector being tangent to the focusing circle at $45^\circ 2\theta$ the change in the error for $\alpha = 0.5^\circ$ from $2\varphi = 40^\circ$ to $2\varphi = 50^\circ$ is $-.033^\circ$ to $-.016^\circ$, respectively. These are large enough for a correction to be necessary in many studies at this diffractometer radius of 14.55 cm. The error decreases as 2φ increases as expected.

In summary, the defocusing error is small in the measurement of residual stress using the PSD and it is not necessary to apply mathematical corrections, especially if the x-ray tube is aligned properly so that the term $\langle y_s \rangle$ is small. Correspondingly, the

error will be small for high angle peaks in any reflection experiment. The equations presented allow for an evaluation of this error in most experimental arrangements, for any linear PSD, with x-rays or neutrons.

5. ACKNOWLEDGEMENTS

The authors would like to thank ONR for support of this work. Portions of this work were submitted in partial fulfillment of the requirements of the Ph.D. degree at Northwestern University in January, 1977 (by M. J.).

REFERENCES

Borkowski, C. J. and Kopp, M. K. (1968). Rev. Sci. Instr. 39, 1515-1522.

Cullity, B. D. (1978), "Elements of X-ray Diffraction," Addison-Wesley, Reading, Mass.

James, M. R. and Cohen, J. B. (1976). Adv. in X-ray Analysis, 19, 697-708.

James, M. R. and Cohen, J. B. (1977). Adv. in X-ray Analysis, 20, 291-308.

James, M. R. and Cohen, J. B. (1978). J. Testing and Evaluation, 6, 91-97.

Zantopulos, H. and Jatczak, C. (1970). Adv. in X-ray Analysis, 14, 360-376.

SAE Handbook Supplement, J784A, 2nd ed., Society of Automotive Engineers, Inc., New York (1971).

Wilson, A. J. C. (1963). "Mathematical Theory of X-ray Powder Diffractometry," Philips Technical Library, Eindhoven, The Netherlands.

TABLE 1

Angles for

$\langle x_s \rangle = \langle y_s \rangle = \langle y_f \rangle = 0$

$2\varphi^\circ$ (true angle)	ψ° (sample tilt)	α° (half divergence angle)	$2\theta^\circ$ (measured angle)	α° (half divergence angle)	$2\theta^\circ$ (measured angle)	α° (half divergence angle)	$2\theta^\circ$ (measured angle)
150	0.0	0.5	149.998	1.0	149.991	2.0	149.963
156	0.0	0.5	155.998	1.0	155.993	2.0	155.970
160	0.0	0.5	159.999	1.0	159.994	2.0	159.975
150	45.0	0.5	149.999	1.0	149.997	2.0	149.989
156	45.0	0.5	155.999	1.0	155.997	2.0	155.989
160	45.0	0.5	155.999	1.0	159.997	2.0	159.989
150	60.0	0.5	150.000	1.0	149.999	2.0	149.996
156	60.0	0.5	156.000	1.0	155.999	2.0	155.995
160	60.0	0.5	160.000	1.0	159.999	2.0	155.994

TABLE 2

Angles for

$\langle x_s \rangle = \langle y_f \rangle = .05$ mm, $\langle y_s \rangle = .25$ mm

$2\varphi^\circ$ (true angle)	ψ° (sample tilt)	α° (half divergence angle)	$2\theta^\circ$ (measured angle)	α° (half divergence angle)	$2\theta^\circ$ (measured angle)	α° (half divergence angle)	$2\theta^\circ$ (measured angle)
150	0.0	0.5	149.998	1.0	149.991	2.0	149.963
156	0.0	0.5	155.998	1.0	155.993	2.0	155.970
160	0.0	0.5	159.999	1.0	159.994	2.0	159.975
150	45.0	0.5	149.977	1.0	149.975	2.0	149.967
156	45.0	0.5	155.983	1.0	155.980	2.0	155.972
160	45.0	0.5	159.986	1.0	159.984	2.0	159.975
150	60.0	0.5	149.962	1.0	149.962	2.0	149.959
156	60.0	0.5	155.969	1.0	155.968	2.0	155.964
160	60.0	0.5	159.974	1.0	159.973	2.0	155.969

TABLE 3

Angles for

$\langle x_s \rangle = \langle y_f \rangle = .05$ mm $\quad \langle y_s \rangle = .25$mm

$2\varphi^o$ (true angle)	ψ^o (sample tilt)	α^o (half divergence angle)	$2\theta^o$ (measured angle)	α^o (half divergence angle)	$2\theta^o$ (measured angle)	α^o (half divergence angle)	$2\theta^o$ (measured angle)
135	0	0.5	134.996	1.0	134.986	2.0	134.943
139	0	0.5	138.997	1.0	138.987	2.0	138.948
143	0	0.5	142.997	1.0	142.988	2.0	142.953
135	45	0.5	134.965	1.0	134.963	2.0	134.957
139	45	0.5	138.968	1.0	138.966	2.0	138.960
143	45	0.5	142.971	1.0	142.970	2.0	142.962
135	60	0.5	134.948	1.0	134.948	2.0	134.947
139	60	0.5	138.951	1.0	138.951	2.0	138.950
143	60	0.5	142.955	1.0	142.955	2.0	142.953

TABLE 4

Angles for

$\langle x_s \rangle = \langle y_s \rangle = \langle y_f \rangle = 0, \quad \psi = 0^o$

detector tangent at	$2\varphi^o$ (true angle)	α^o (half divergence angle)	$2\theta^o$ (measured angle)	α^o (half divergence angle)	$2\theta^o$ (measured angle)
45^o	40	0.5	39.967	1.0	39.868
	45	0.5	44.979	1.0	44.916
	50	0.5	49.984	1.0	49.938
70^o	65	0.5	64.986	1.0	64.943
	70	0.5	69.988	1.0	69.950
	75	0.5	74.989	1.0	74.955
85^o	80	0.5	79.990	1.0	79.958
	85	0.5	84.991	1.0	84.962
	90	0.5	89.991	1.0	89.965

FIGURE CAPTIONS

FIGURE 1 Geometry of the focusing error on a powder diffractometer.

FIGURE 2 Illustration of the terms used in the calibration of the PSD. The term 2φ represents the angular range covered by the detector, nz is the total number of channels and α is the angular increment for one channel, near the point of tangency of the PSD to the focusing circle.

FIGURE 3 Co-ordinates employed in the text for a powder diffractometer.

FIGURE 4 The angles of diffraction for the left and right divergent rays.

FIGURE 5 Geometry for the location of the position sensitive detector.

FIGURE 6 Geometry for x_r at $\psi = 0^o$.

FIGURE 7 Geometry for y_r at $\psi = \psi^o$. The terms β_L and β_r describe the angle between the j axis and a line connecting the origin and the intersection of the left and right diffracted beams with the PSD.

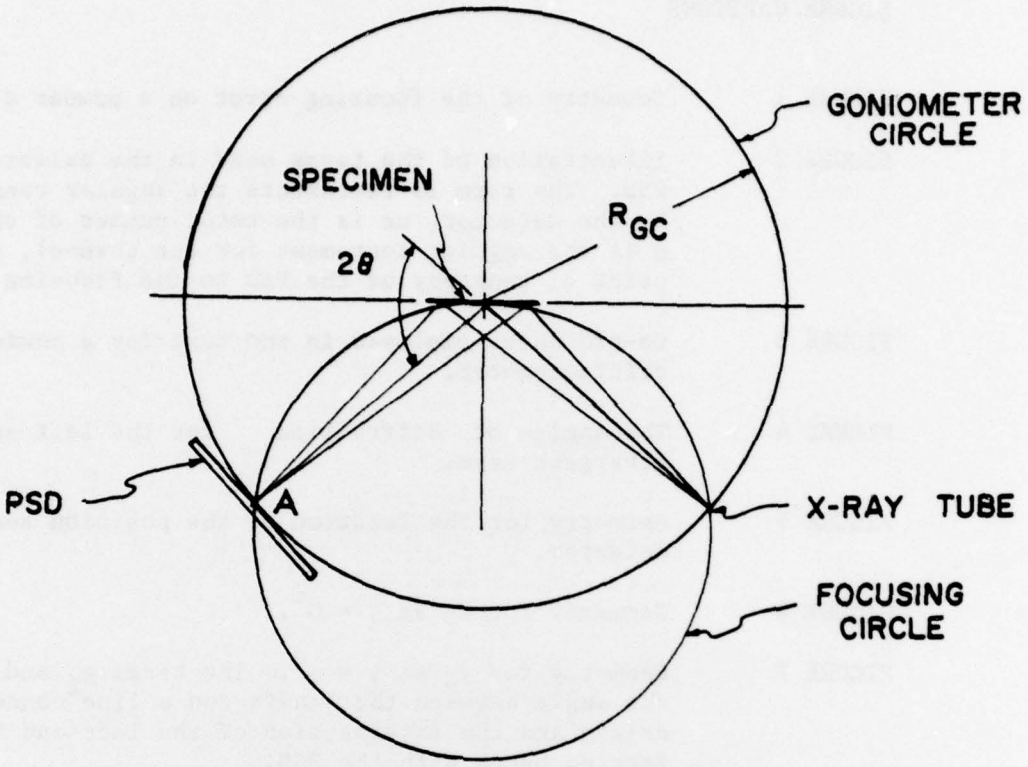

a. $\psi = 0°$

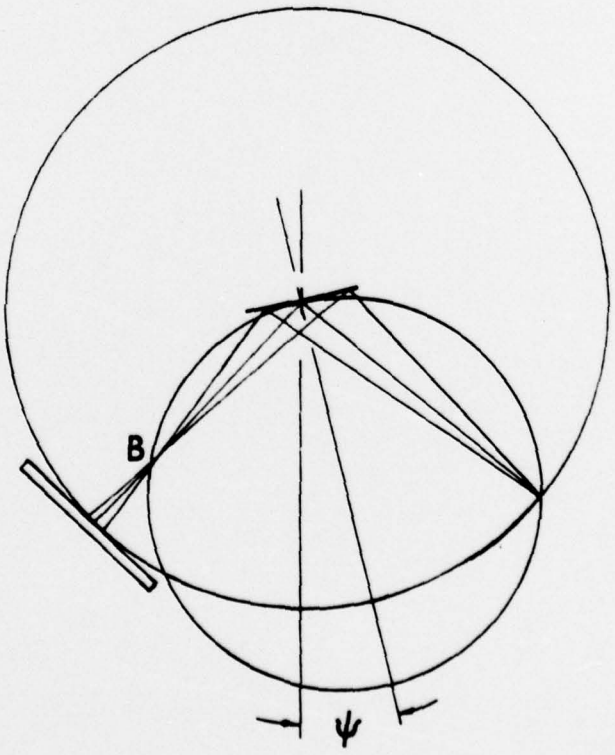

b. $\psi = \psi°$

FIGURE 1

(M. R. James & J. B. Cohen)

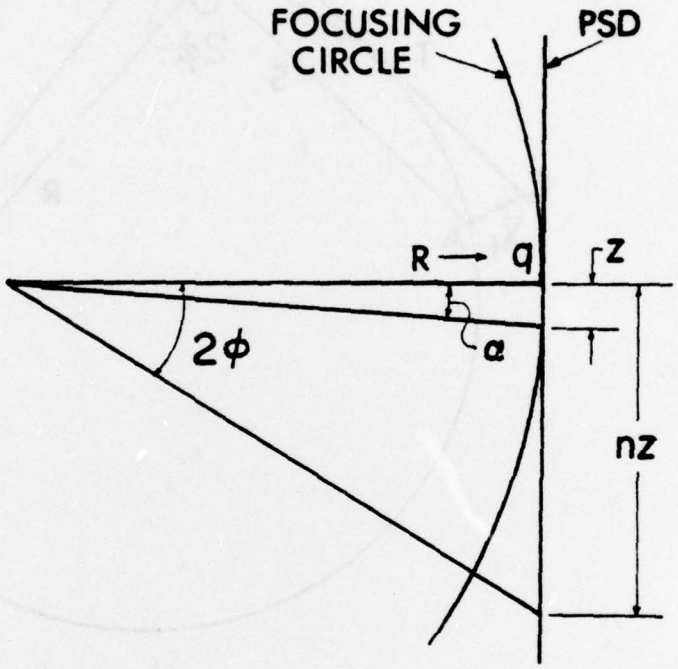

FIGURE 2

(M. R. James & J. B. Cohen)

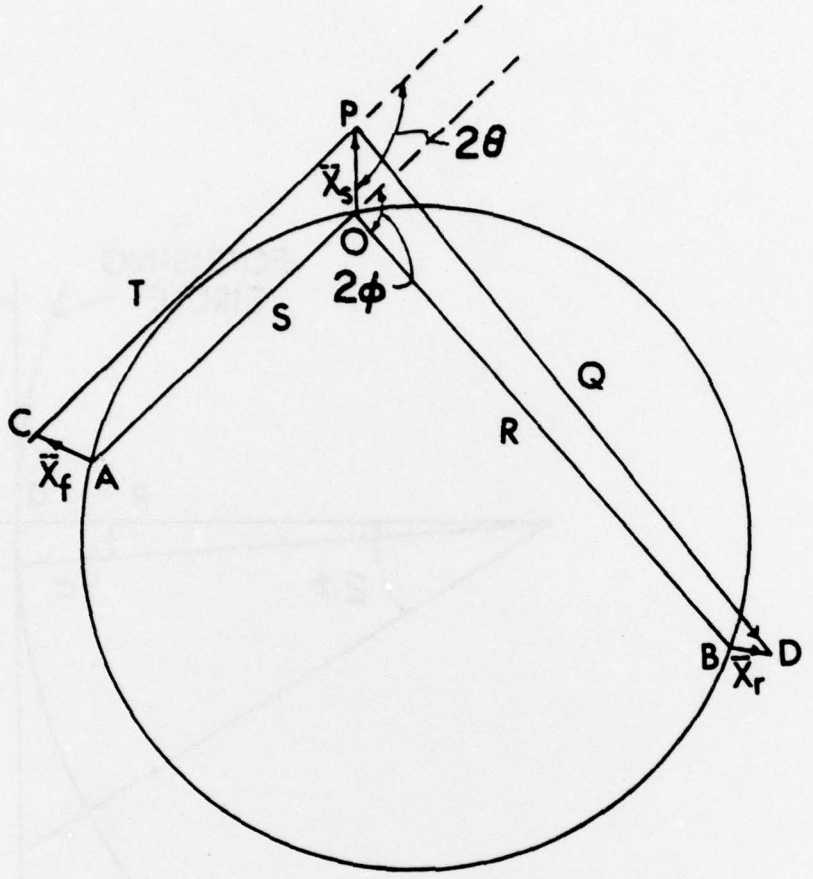

FIGURE 3.

(M. R. James and J. B. Cohen)

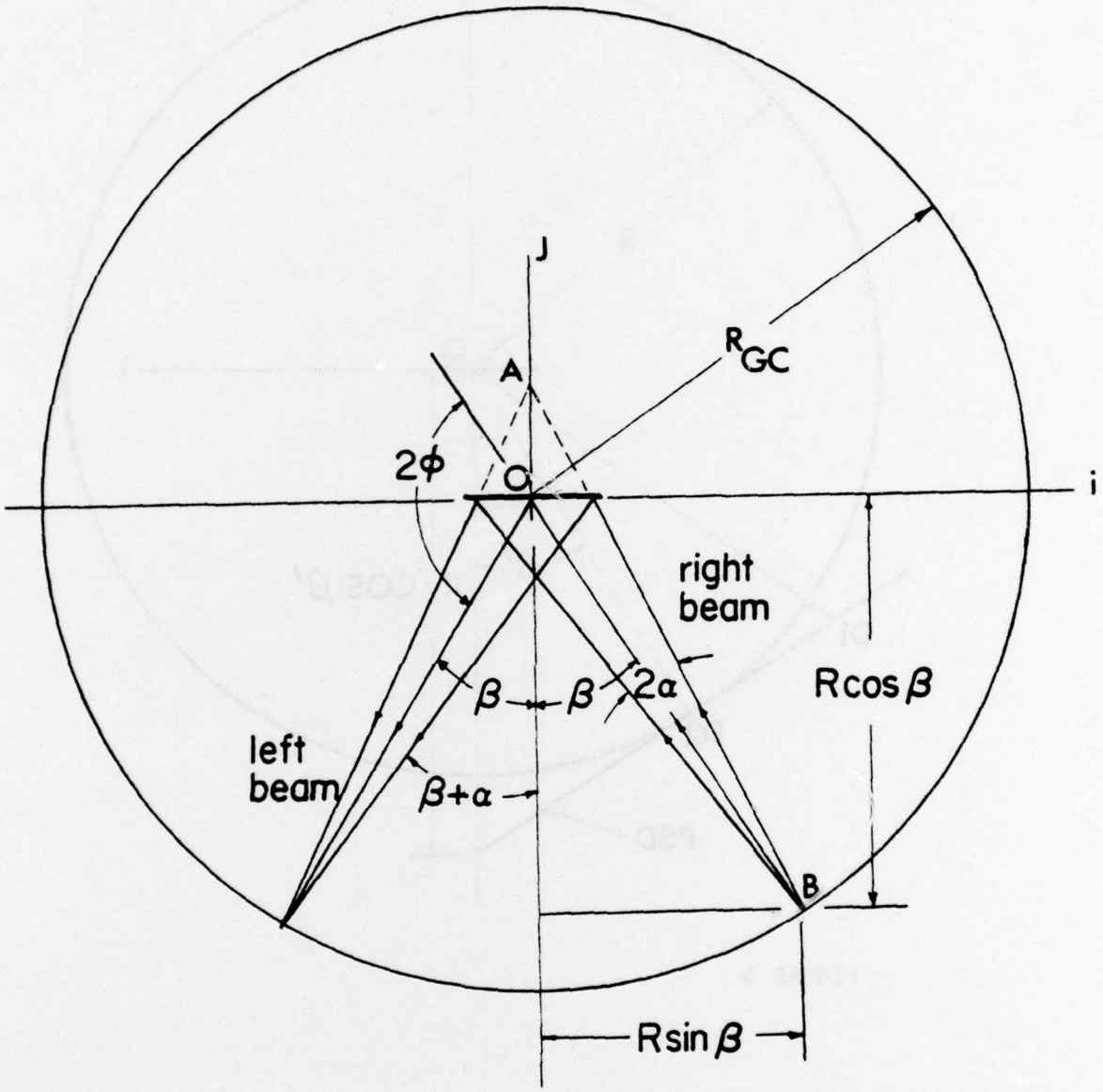

FIGURE 4

(M. R. James and J. B. Cohen)

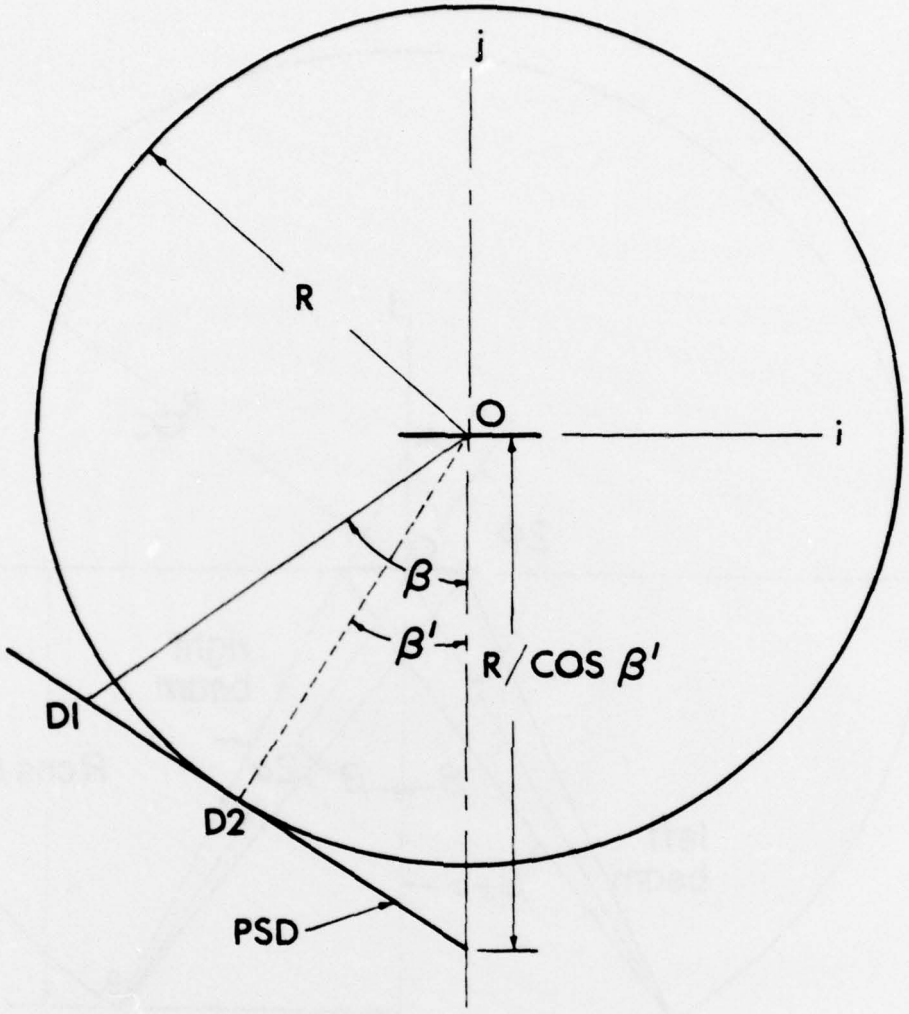

FIGURE 5

(M. R. James and J. B. Cohen)

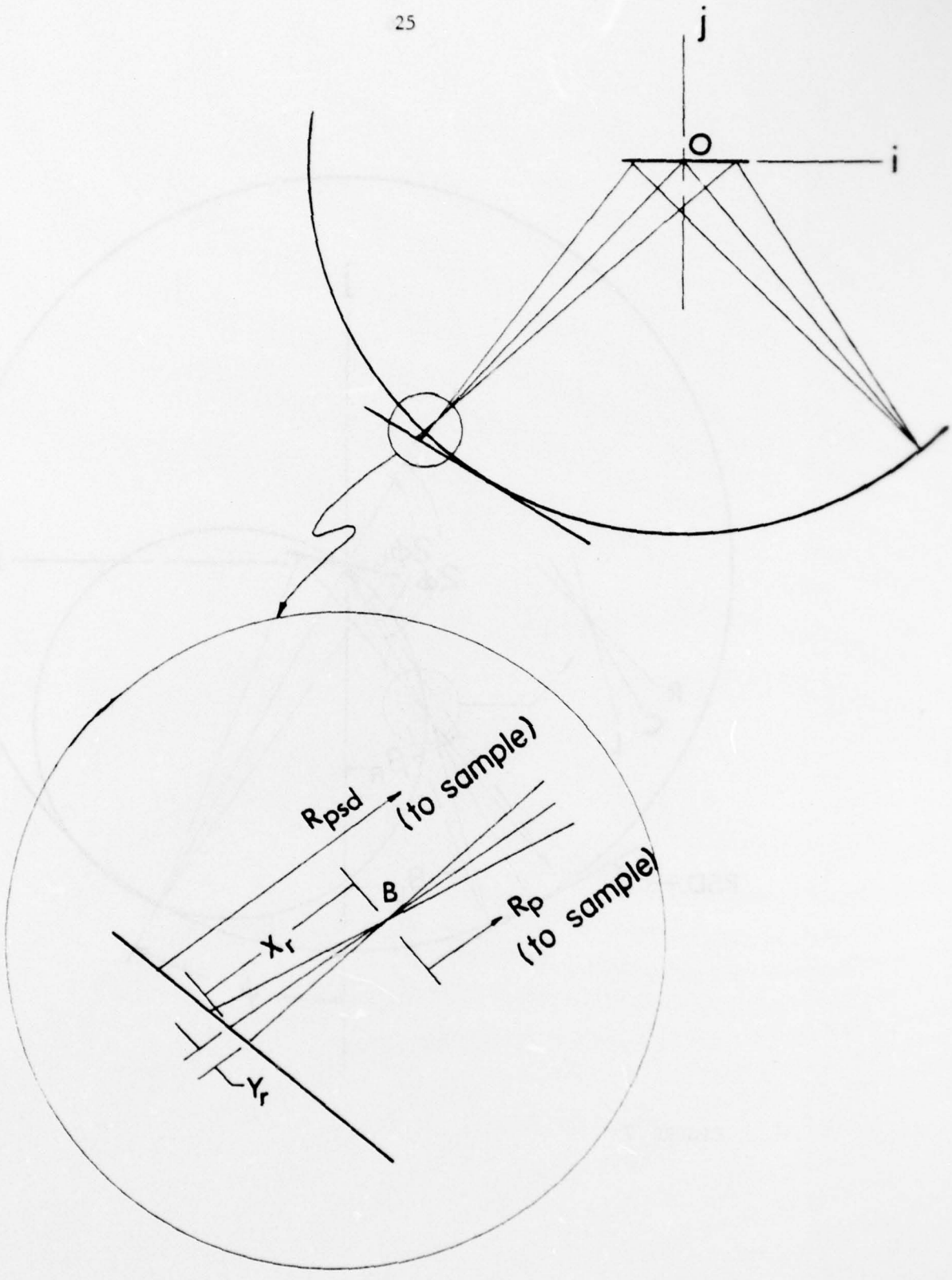

FIGURE 6

(M. R. James and J. B. Cohen)

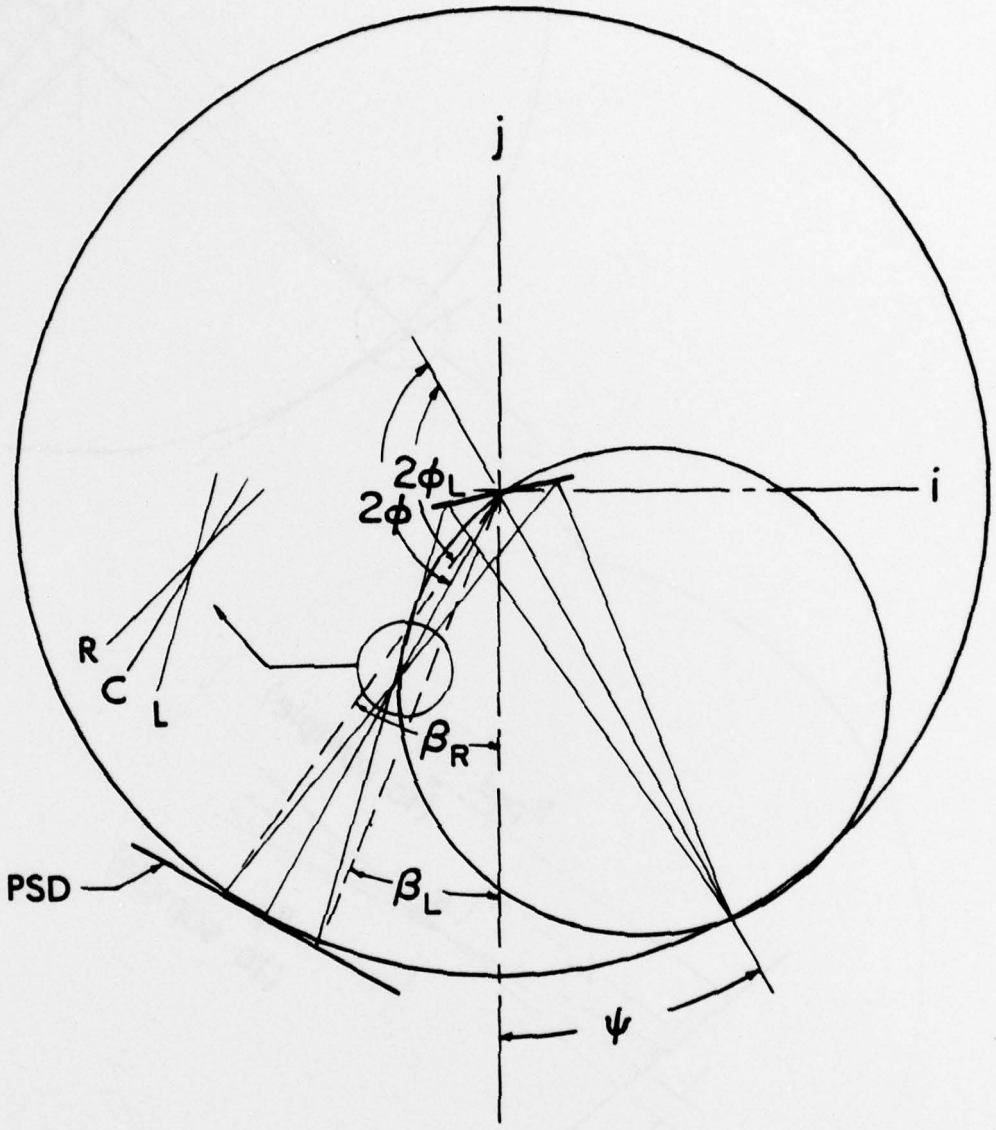

FIGURE 7

(M. R. James and J. B. Cohen)

Unclassified

Security Classification

DOCUMENT CONTROL DATA - R & D

Security classification of title, body of abstract and indexing annotation must be entered when the overall report is classified)

1. ORIGINATING ACTIVITY (Corporate author)

Jerome B. Cohen, Northwestern University, Evanston, Illinois

2a. REPORT SECURITY CLASSIFICATION

Unclassified

2b. GROUP

3. REPORT TITLE

GEOMETRICAL PROBLEMS WITH A POSITION SENSITIVE DETECTOR EMPLOYED ON A DIFFRACTOMETER, INCLUDING ITS USE IN THE MEASUREMENT OF STRESS

4. DESCRIPTIVE NOTES (Type of report and inclusive dates)

Technical Report No. 20

5. AUTHOR(S) (First name, middle initial, last name)

Michael R. James and Jerome B. Cohen

6. REPORT DATE	7a. TOTAL NO. OF PAGES	7b. NO. OF REFS
June 16, 1978	26	8

8a. CONTRACT OR GRANT NO.	9a. ORIGINATOR'S REPORT NUMBER(S)
N00014-75-C-0580 NR 031-733	Technical Report No. 20
b. PROJECT NO. 5345-455	
c.	9b. OTHER REPORT NO(S) (Any other numbers that may be assigned this report)
d.	None

10. DISTRIBUTION STATEMENT

Distribution of this document is unlimited.

DISTRIBUTION STATEMENT A
Approved for public release; Distribution Unlimited

11. SUPPLEMENTARY NOTES	12. SPONSORING MILITARY ACTIVITY
	Office of Naval Research Metallurgy Branch

13. ABSTRACT

Defocusing errors associated with the use of a straight one dimensional position sensitive detector on a powder diffractometer are examined. At high angles, the error is less than the resolution of currently available detectors for x-rays.

DD FORM 1 NOV 65 1473 (PAGE 1)

S/N 0101-807-6801

Unclassified

Security Classification

14 KEY WORDS	LINK A		LINK B		LINK C	
	ROLE	WT	ROLE	WT	ROLE	WT
position sensitive detector (PSD) geometric errors with PSD's on a diffractometer geometric errors - PSD's used to measure stress						